scientific reports

Check for updates

OPEN

Prognostic assessment of early-stage liver cirrhosis induced by HCV using an integrated model of CX3CR1-associated immune infiltration genes

Haozheng Cai[1,4], Jing Zhang[3,4], Chuwen Chen[1], Junyi Shen[1], Xiaoyun Zhang[1], Wei Peng[1], Chuan Li[1], Haopeng Lv[2] & Tianfu Wen[1]✉

Chemokine (C-X3-C motif) Receptor 1 (CX3CR1) primarily mediates the chemotaxis and adhesion of immune cells. However, its role in hepatitis C virus (HCV)-induced early-stage liver cirrhosis remains unexplored. GSE15654 was downloaded from the GEO database. The Cox regression model, CIBERSORT, and LASSO technique were utilized to identify CX3CR1-associated immune infiltration genes (IIGs). Surgical resection samples were collected for verification, including 3 healthy controls (HC), 4 individuals with HCV-induced hepatic cirrhosis, and 3 with HCV-induced liver failure. High CX3CR1 expression correlated with worse prognosis in early-stage cirrhosis. CX3CR1-associated IIGs, namely ACTIN4, CD1E, TMCO1, and WSF1, were identified, showing specific expression in the livers of individuals with post-hepatic cirrhosis and liver failure compared to HC. LOC400499 and MTHFD2 were elevated in individuals with liver failure in comparison to those with hepatocirrhosis. Notably, high infiltration of plasma cells and low infiltration of monocytes were predictive of poor prognosis in early-stage cirrhosis. The combined risk model predicted that high expression of CX3CR1-associated IIGs and increased infiltration of plasma cells were associated with unfavorable prognosis in individuals with HCV-induced early-stage liver cirrhosis. The developed combined risk model effectively predicted the prognosis of these individuals.

Keywords HCV, Liver fibrosis, CX3CR1, Immune, Prognosis

Liver cirrhosis is a common physiological outcome of chronic fibrotic liver disease caused by various factors[1,2]. It involves the replacement of normal hepatic architecture with regenerative hepatic nodules[3]. Hepatitis C virus (HCV) affects around 71 million individuals and is a major cause of liver cirrhosis [4,5]. The considerable genetic diversity of HCV has led to the identification of eight genotypes and various subtypes, especially in certain geographical regions, with genotypes 1 and 3 being the most prevalent globally[6]. Study has demonstrated a correlation between HCV genotypes and viral load, with genotype 1 typically associated with higher viral loads. Elevated viral loads are often linked to an increased risk of cirrhosis[7]. Liver cirrhosis claims approximately 1 million lives annually worldwide, ranking it as the 11th leading cause of mortality[2]. Diagnosing liver fibrosis during the asymptomatic compensatory period remains challenging[8,9], leading many individuals to miss early treatment opportunities. In addition, there are no effective methods to reverse cirrhosis[10]. Thus, there is an urgent need for new diagnostic techniques to accurately detect early-stage liver fibrosis and identify effective therapeutic targets to slow its progression.

Chemokine (C-X3-C motif) Receptor 1 (CX3CR1) is predominantly expressed in monocytes, macrophages, a subset of NK cells, and terminally differentiated cytotoxic T cells[11]. Its primary function involves mediating the chemotaxis and adhesion of immune cells by binding with its unique ligand CX3CL1[11]. Several studies have demonstrated that increased expression of CX3CR1 contributes to the deterioration of obstruction-induced kidney fibrosis[10] and is correlated with a worse prognosis in individuals with idiopathic pulmonary fibrosis[12].

[1]Division of Liver Surgery, Department of General Surgery, West China Hospital, Si Chuan University, Chengdu 610041, China. [2]Department of General Surgery, ChengDu Shi Xinjin Qu Renmin Yiyuan: People's Hospital of Xinjin District, Chengdu, China. [3]Division of Biliary Tract, Department of General Surgery, West China Hospital, Si Chuan University, Chengdu, China. [4]These authors contributed equally to this work. ✉email: wentianfu@scu.edu.cn

However, regarding liver cirrhosis, the role of CX3CR1 is controversial. While one study showed significantly increased expression of CX3CR1 in end-stage liver fibrosis induced by chronic hepatitis C[13], another study suggested that overexpression of CX3CR1 could alleviate liver inflammation and fibrosis in the carbon tetrachloride (CCl4)-induced fibrosis model[14]. Presently, no research has confirmed the involvement of CX3CR1 in predicting the prognosis of liver cirrhosis. Therefore, the primary objective of this research was to determine the link between CX3CR1 and the prognosis of individuals with early hepatic fibrosis induced by HCV.

Liver fibrosis occurs through iterative cycles of tissue injury, inflammation, and repair, in a microenvironment of cytokines and chemokines, where the interaction among the innate and adaptive immune systems and stromal cells leads to hepatic stellate cell (HSC) activation and extracellular matrix (ECM) accumulation, ultimately results in liver cirrhosis[15,16]. The infiltration pattern of immune cells in the liver significantly influences the advancement of liver fibrosis[17]. As mentioned earlier, CX3CR1 is a key mediator of immune cell migration during organ fibrosis. Some studies have indicated that the level of CX3CR1 in M1 macrophages in bronchoalveolar lavage fluid is significantly higher in mice with interstitial lung disease[12,18], and inhibiting the expression of CX3CR1 in BALF reduces M1 macrophage infiltration[18]. In peritoneal fibrosis, CX3CR1 mediates the expression of CX3CL1 and TGF-β on the peritoneal mesothelium, promoting the development of peritoneal fibrosis[19]. However, the association between CX3CR1 and immune cell infiltration remains unclear in HCV-induced early-stage liver fibrosis.

In the current research, the prognostic value of CX3CR1 was innovatively explored in individuals with chronic HCV-induced early-stage liver cirrhosis, and the link between CX3CR1 and immune cell infiltration was analyzed using bioinformatic analysis. An integrated model was developed for predicting the prognosis of these individuals based on the expression of CX3CR1, CX3CR1-associated immune infiltration genes (IIGs), and immune cell infiltration. Furthermore, clinical samples were collected from healthy liver donors, individuals with compensated cirrhosis, and those with acute-on-chronic liver failure to verify the findings. PCR primer sequences are listed in Table 1. In summary, the research proposes that CX3CR1 can potentially be targeted to prevent and address the progression of liver cirrhosis in the future.

Results

High expression of CX3CR1 predicts poor prognosis in individuals with liver cirrhosis

The bioinformatic analysis flowchart and methodologies employed in the research are given in Fig. 1. The clinical information of patients from public database was presented in Table 2. Based on the expression of CX3CR1, 216 individuals were divided into two categories using maximally selected rank statistics, yielding 186 cases in the high-risk and 30 cases in the low-risk category (Fig. 2a and b). Survival analysis demonstrated that individuals in the high-risk category exhibited significantly shorter survival compared to those in the low-risk category, as illustrated by the risk curves, which show a marked difference in survival rates over time between the two groups ($P = 0.011$). The median survival time (MST) for the high-risk group is 4591 days (Fig. 2c). The clinical details of Model 1 are shown in Table 3.

Gene	Bidirectional primer sequence	Product length (bp)
β-actin(H)	F:5′GTGGCCGAGGACTTTGATTG3′ R:5′CCTGTAACAACGCATCTCATATT3′	73
ACTN4	F:5′TGATCTGGACCATCATCCTTAG3′ R:5′TTCTGCACATTGACGTTCTTAT3′	127
BRWD1	F:5′CTCTCATCGAGTCGGAGCTGT3′ R:5′CAGTCCAATCTCTTCGGCAAC3′	127
CD1E	F:5′TGAAGAAGTGGAAGACACGC3′ R:5′AAAATCTCTGGAAGATGGGG3′	191
HYPK	F:5′ATTGCCCTAACCAACTGATGC3′ R:5′CCAGATGTACCTTGAATACTGTTGA3′	297
ITGB7	F:5′CTTTGCCAATGGTCCTTGTTTT3′ R:5′ACGCGGTGAAGTTCAGTTGC3′	207
LOC400499	F:5′CCTATCATTTTTCCACCAACACC3′ R:5′AAGACCACTCCCCTCCACCA3′	65
MTHFD2	F:5′CAAGTCACTCCTATGTCCTCAAC3′ R:5′CCTTCTCTCATCAATATGCTCTG3′	191
THBS2	F:5′GGACGAGCCCTTCTACGA3′ R:5′TTGCTGGCAACCCTTCTT3′	160
TMCO1	F:5′TTTTACTGCCCTAATGGGAATG3′ R:5′CGATGAGACAGTCCTTGGATGTA3′	102
TMPRSS13	F:5′CTGTTCGCTGTGACGGGGT3′ R:5′TTTCCTGGATGGTGGAGTTGTAT3′	270
WFS1	F:5′CCCAAGAAGAAGAAGCAGGTG3′ R:5′CCCTTGGCGTACTTCTTAGTGAT3′	206

Table 1. PCR primer sequences. PCR, polymerase chain reaction; ACTN4, alpha-actinin 4, BRWD1, bromodomain and WD repeat-containing protein 1, HYPK, Huntingtin yeast partner K, MTHFD2, Methylenetetrahydrofolate dehydrogenase 2, THBS2, ECM protein thrombospondin-2, TMCO1, transmembrane and coiled-coil domains 1, TMPRSS13, transmembrane protease serine 13.

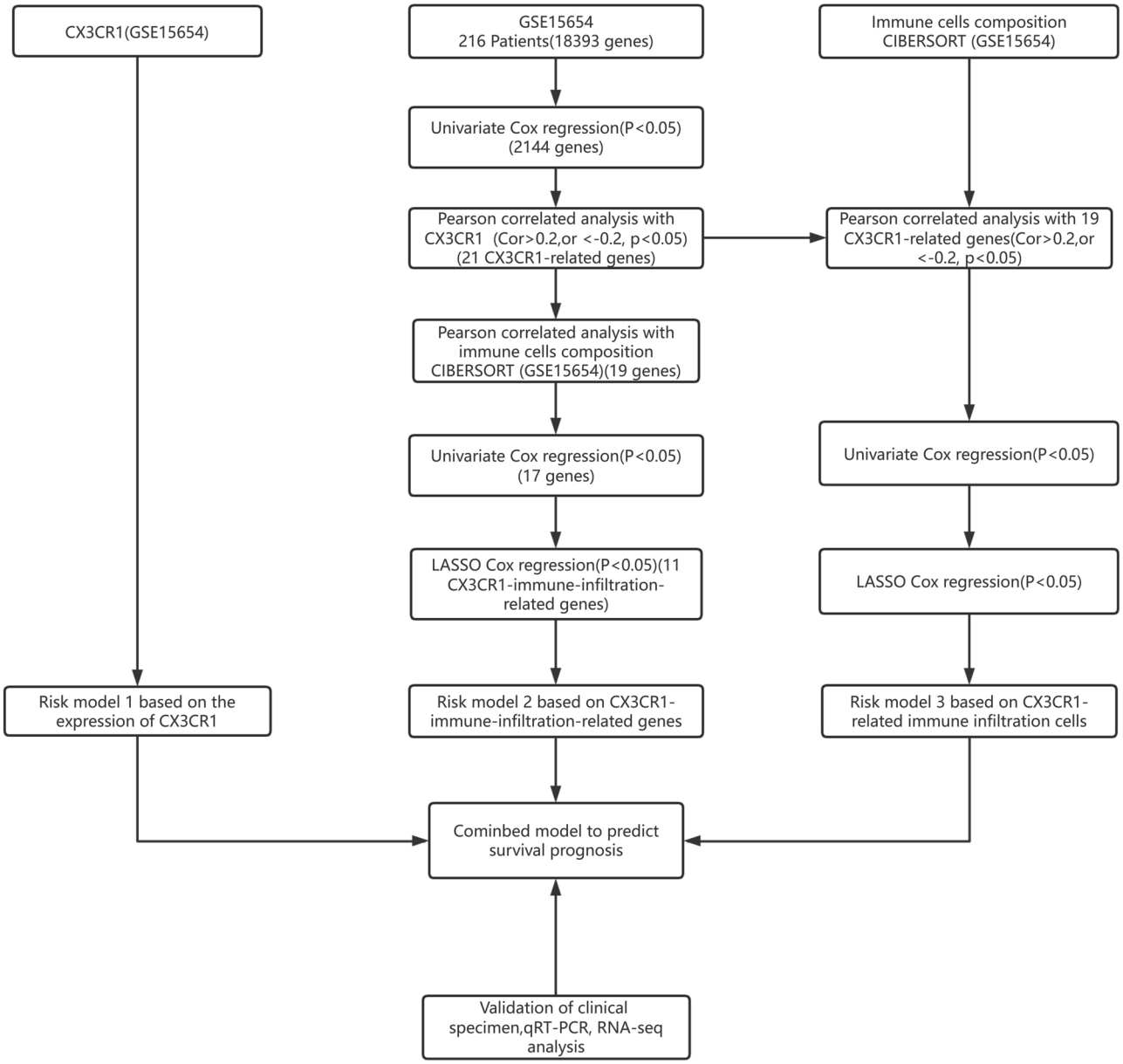

Fig. 1. The flow-chart and methodologies of the research.

Characteristics	GSE15654 (n = 216)
Survival	150(69.44%)
HCC	65(30.09%)
Child–pugh class B/C	66(30.56%)
Platelet < 100,000/mm^3	99(45.83%)

Table 2. Clinical information of patients.

CX3CR1-associated genes and their function in liver cirrhosis

From a pool of 18,393 genes, 2114 genes were identified using univariate Cox regression analysis. Subsequently, 21 genes linked to CX3CR1 expression were isolated from the initial 2114 genes using Pearson correlation analysis, as depicted in the correlation heatmap (Fig. 2d). Functional analysis revealed that CX3CR1-associated genes were prominently associated with endoplasmic reticulum (ER) calcium ion homeostasis and ER overload response within the biological process (BP). Cellular component (CC) analysis showed that CX3CR1-associated genes were mainly enriched in the integral component of the ER membrane. Molecular function (MF) analysis

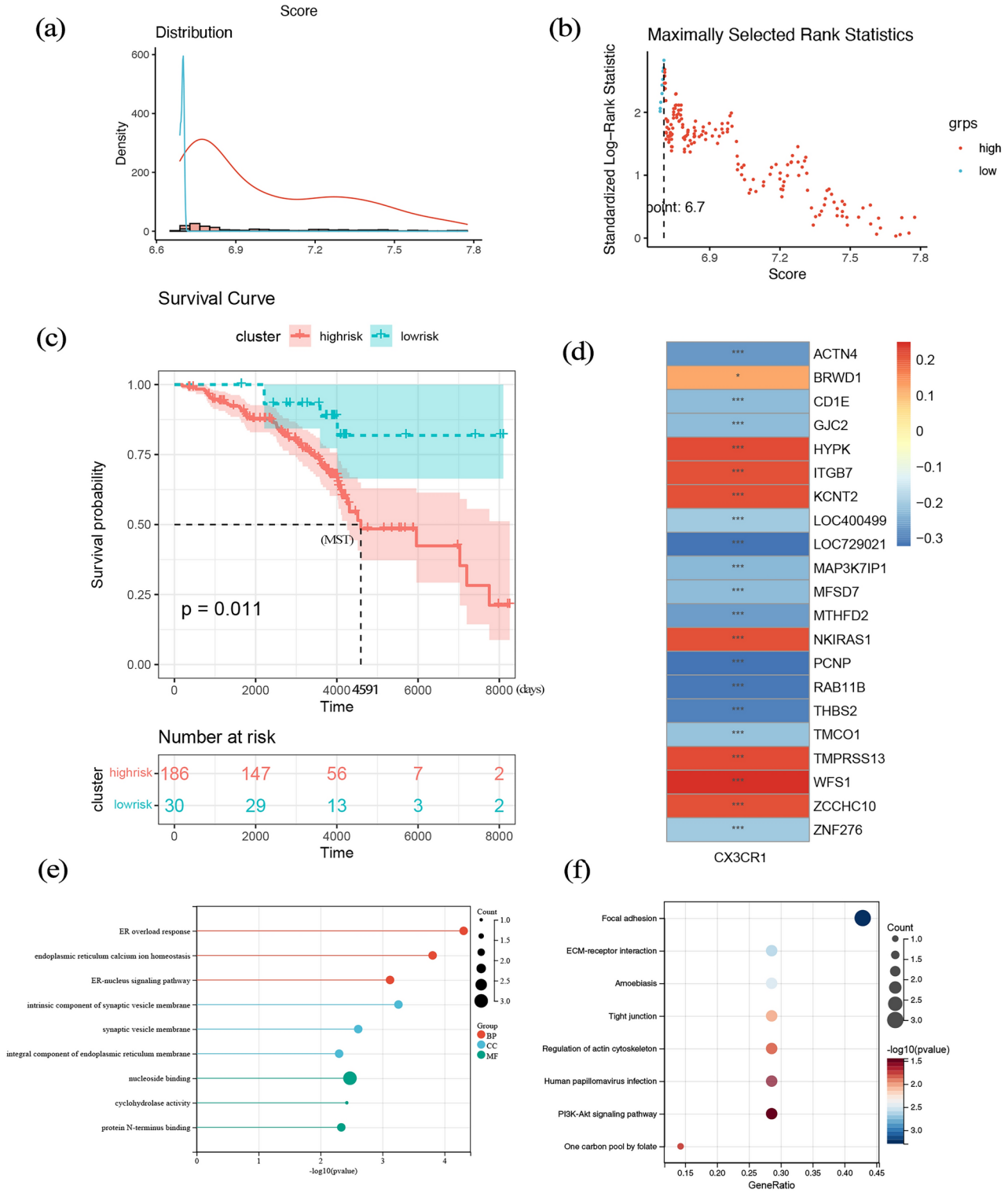

Fig. 2. (**a**) Histogram based on maximally selected rank grouping in model1. (**b**) Grouping cut-off value based on maximally selected rank. (**c**) Kaplan–Meier diagram of the total survival rate of Model1. (**d**) Heatmap showed the correlations between CX3CR1 and genes which screened by univariate Cox analysis from whole genome. (**e**) Lollipop chart showed the GO function enrichment of CX3CR1 related genes. (**f**) Bubble diagram of KEGG pathway of CX3CR1 related genes.

Model 1	High-risk group (186)	Low-risk group (30)
Survival	124(66.67%)	26(86.67%)
Survival time(days, mean ± s.d.)	3264.45 ± 1502.02	4046.97 ± 1518.64
Platelet < 100,000/mm^3	88(47.31%)	11(36.67%)
HCC	60(32.26%)	5(16.67%)
Child–Pugh class B/C	59(31.72%)	7(23.33%)
Model 2	**High-risk group (96)**	**Low-risk group (120)**
Survival	47(48.96%)	103(85.83)
Survival time(days, mean ± s.d.)	2978.14 ± 1473.80	3689.12 ± 1497.24
Platelet < 100,000/mm^3	51(53.12%)	48(40.00%)
HCC	34(35.42%)	31(25.83%)
Child–Pugh class B/C	43(44.79%)	23(19.17%)
Model 3	**High-risk group (23)**	**Low-risk group (193)**
Survival	9(39.13%)	141(73.06%)
Survival time(days, mean ± s.d.)	2593.35 ± 1458.58	3466.06 ± 1509.72
Platelet < 100,000/mm^3	11(47.82%)	88(45.60%)
HCC	11(47.82%)	54(27.98%)
Child–Pugh class B/C	13(56.52%)	53(27.46%)
Combined model	**High-risk group (121)**	**Low-risk group (95)**
Survival	62(51.24%)	88(92.63%)
Survival time(days, mean ± s.d.)	3407.96 ± 1449.39	3787.31 ± 1526.00
Platelet < 100,000/mm^3	64(52.89%)	35(36.84%)
HCC	44(36.36%)	21(22.11%)
Child–Pugh class B/C	50(41.32%)	16(16.84%)

Table 3. Clinical information of patients in different model.

indicated their substantial association with protein N-terminus binding (Fig. 2e). Furthermore, KEGG pathway analysis revealed that CX3CR1-associated genes were enriched in amoebiasis, extracellular matrix (ECM)–receptor interaction, and related processes (Fig. 2f). KEGG imagery is used with permission from the Kanehisa laboratory[20].

CX3CR1-associated immune infiltration genes and their prognostic correlation in individuals with liver cirrhosis

In the discovery dataset, CIBERSORT was employed for the identification of the composition of 22 immune cell types. Using Pearson correlation analysis, a CX3CR1-associated gene correlated with immune cell infiltration was identified (Fig. 3a). Further, univariate Cox regression and LASSO Cox regression analyses were employed to filter genes, identifying 11 optimal prognostic genes known as CX3CR1-associated IIGs (Fig. 3b and c). Based on the expression and corresponding coefficients of 11 CX3CR1-associated IIGs, risk score 2 was computed utilizing the following equation: expression of ACTIN4 × 1.106 + expression of BRWD1 × (− 0.477) + expression of CD1E × 0.328 + expression of HYPK × (− 0.951) + expression of ITGB7 × (− 0.474) + expression of LOC400499 × 0.234 + expression of MTHFD2 × 0.173 + expression of THBS2 × 0.335 + expression of TMCO1 × (− 0.629) + expression of TMPRSS13 × (− 1.376) + expression of WES1 × (− 0.382). Applying risk score 2, the maximally selected rank method divided individuals into high-risk (96 individuals) and low-risk categories (120 individuals) (Fig. 3d). The cut-off value was − 9.49 (Fig. 3e). The forest plot of 11 CX3CR1-associated IIGs is shown in Fig. 3f. Survival analysis demonstrated that the high-risk category had shorter survival times in comparison to the low-risk category ($P < 0.0001$) (Fig. 3g). The MST for the high-risk group is 3822 days. The clinical information of Model 2 is shown in Table 3.

CX3CR1-associated immune infiltration cells and their prognostic significance in individuals with liver cirrhosis

Based on CIBERSORT outcomes, immune cells exhibiting correlation with the expression of CX3CR1 were retained (Fig. 3a). Using univariate Cox regression and LASSO Cox regression analyses, immune cell types were further refined (Fig. 4a and b). Among these, three immune cell types were identified as CX3CR1-associated immune infiltration cells. Formulating risk model 3 involved the following formula: Plasma cells × 4.346 + T follicular helper cells × 9.680 + Monocytes × (− 6.143). Based on the risk score 3, individuals were classified into high-risk (23 individuals) and low-risk categories (193 individuals), with a cut-off value of 0.54 (Fig. 4c and d). The high-risk category exhibited a poor prognosis in comparison to the low-risk category ($P < 0.0001$) (Fig. 4e). The MST for the high-risk group is 3062 days, while for the low-risk group it is 7027 days. The clinical information of Model 3 is shown in Table 3.

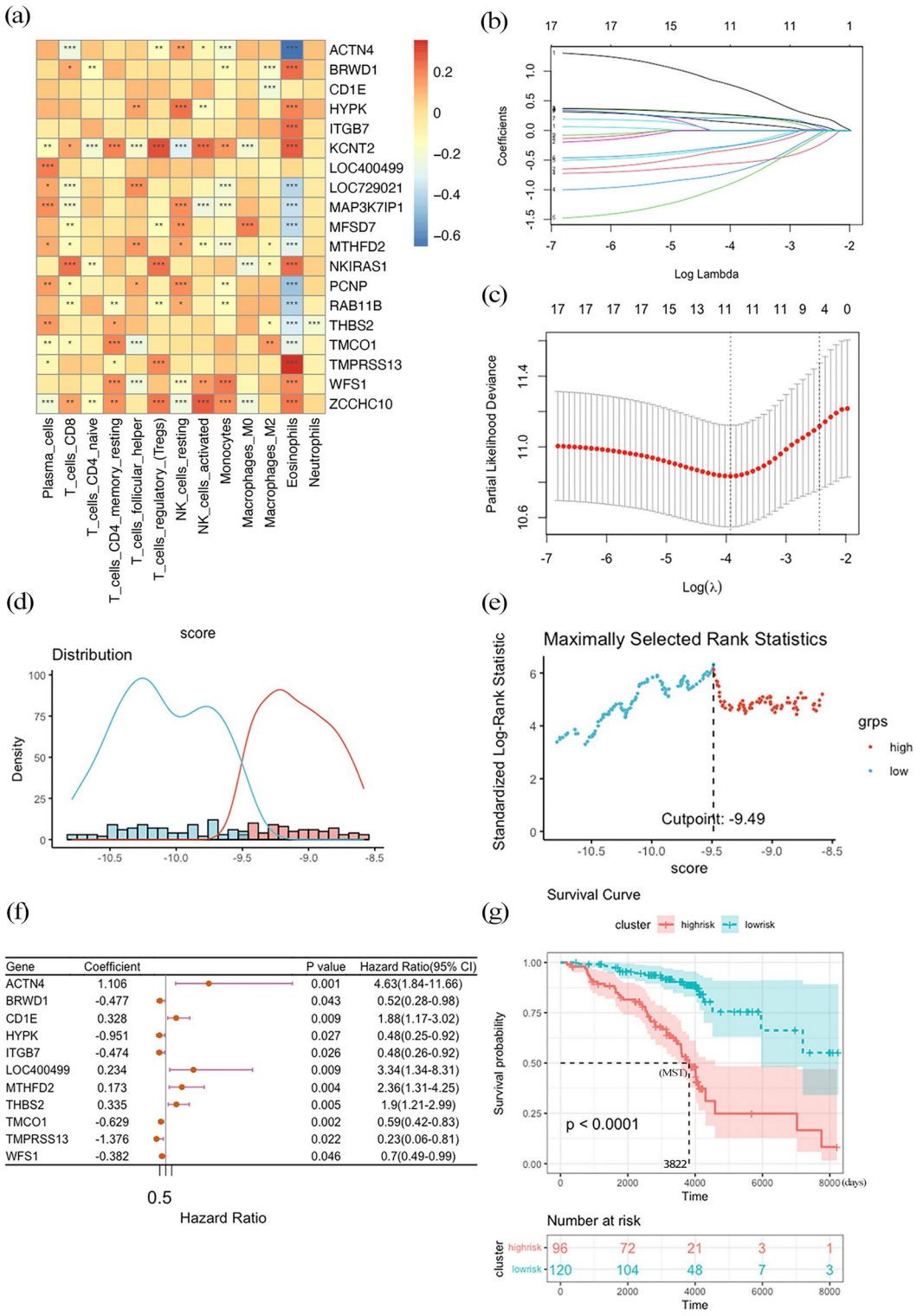

Fig. 3. (**a**) The correlations between the CX3CR1-related genes and immune cell compositions. (*** means $P<0.01$, ** means $P<0.05$, and * means $P<0.1$). (**b**) LASSO coefficient profiles of 11 CX3CR1-related immune infiltration genes. (**c**) Three-fold cross-validation of lasso analysis. Error bars represented the SE. The dotted vertical lines showed the optimal values. (**d**) Histogram based on maximally selected rank grouping in model2. (**e**) Grouping cut-off value based on maximally selected rank. (**f**) Forest plot of 11 CX3CR1-related immune infiltration genes with $P<0.05$ by univariate Cox regression. (**g**) Kaplan–Meier diagram of the total survival rate of Model2.

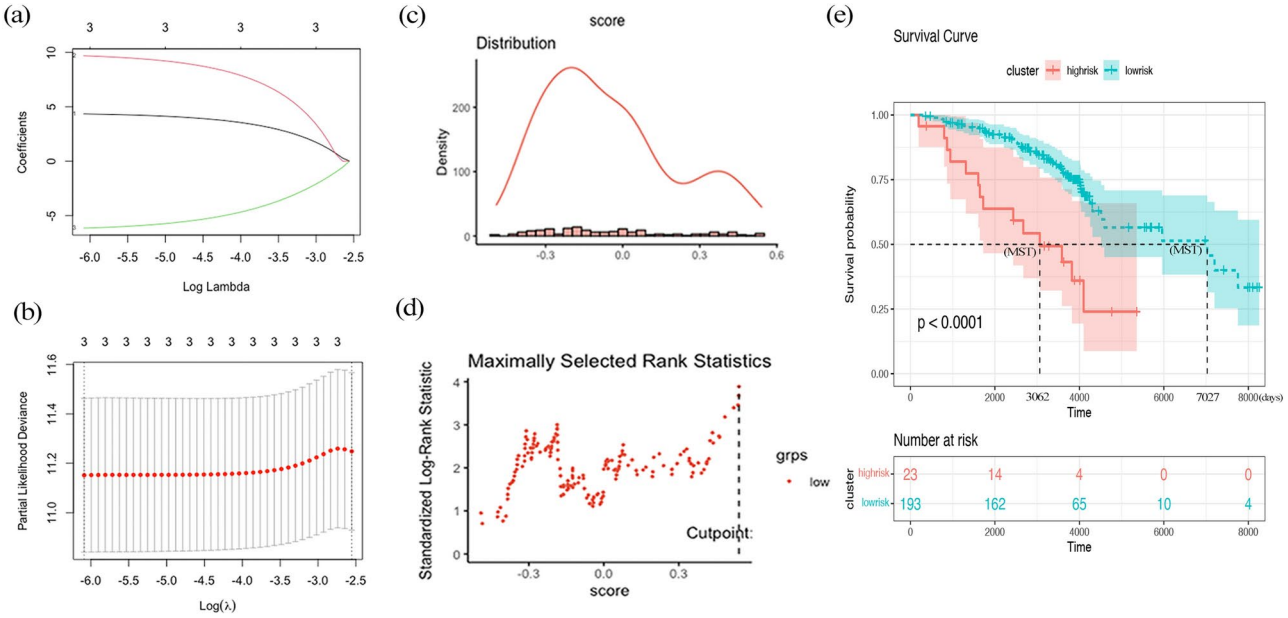

Fig. 4. (**a**) LASSO coefficient profiles of 3 CX3CR1-related immune infiltration cells. (**b**) Three-fold cross-validation of lasso analysis. (**c**) Histogram based on maximally selected rank grouping in model3. (**d**) Grouping cut-off value based on maximally selected rank. (**e**) Kaplan–Meier diagram of the total survival rate of model3.

Integrated prognostic model based on risk scores 1–3 for individuals with liver cirrhosis

To predict patient prognosis, an integrated model was constructed using multivariate Cox regression analysis based on risk models 1–3 (Fig. 5a and b). The combined risk score was derived as follows: Combined risk score = risk score 1×0.6264 + risk score 2×0.9714 + risk score 3×0.3491. According to the maximally selected rank statistics, 121 individuals were placed in the high-risk and 95 in the low-risk category (Fig. 5c and d). Individuals in the high-risk category exhibited a notably shorter overall survival period in comparison to the low-risk category ($P < 0.0001$) (Fig. 5g). In the combined model, the MST for the high-risk group is 4012 days. Individuals in the high-risk category demonstrated higher plasma cell infiltration and lower monocyte infiltration in comparison to the low-risk category (Fig. 5e and f). The clinical information of the combined Model is given in Table 3.

Preliminary validation of clinical samples:

Lower expression levels of ACTN4, TMCO1, CD1E, and WFS1 were observed in the liver tissues of patients compared to normal liver donors. Conversely, the expression levels of LOC400499 and MTHFD2 were elevated in individuals with liver failure in comparison to those with hepatocirrhosis (Fig. 6a). CIBERSORT results indicated that the infiltration level of plasma cells was higher in specimens with liver failure compared to those with hepatic cirrhosis. In contrast, the infiltration of monocytes was lower in the liver failure group (Fig. 6b). This was consistent with the trends observed in our bioinformatics analysis; however, due to the small sample size, it lacked statistical significance. Furthermore, Pearson correlation analysis showed a negative relationship between the expression of BRWD1 and the aspartate aminotransferase levels in patients (Fig. 6c). In addition, the findings demonstrated a positive relationship between the expression of LOC400499 and the levels of total bilirubin (TB) and direct bilirubin (DB) (Fig. 6d and e). Similarly, the expression of MTHFD2 exhibited positive correlations with TB, DB, and indirect bilirubin levels (Fig. 6f–h). The clinical information of patients was presented as Table 4.

Discussion

CX3CR1, the sole receptor for CX3CL1, has been established as pivotal in prior research. The CX3CR1–CX3CL1 axis has been highlighted for its substantial role in liver fibrosis and cirrhosis progression. This study is the first to delineate the significance of CX3CR1 within a retrospective cohort of HCV-induced cirrhosis. The findings showed that high expression of CX3CR1 serves as a risk factor for the prognosis of individuals with HCV-induced cirrhosis. A series of genes and immune cells correlated with the expression of CX3CR1 were identified in the discovery dataset, leading to the successful establishment of the prognosis model. Furthermore, this study was supported by preliminary validation using clinical specimens. The present study not only advances the understanding of therapeutic targets but also furnishes potential prognostic markers for individuals with HCV-induced liver fibrosis and cirrhosis.

At present, the significance of CX3CR1 in liver fibrosis remains controversial. A previous investigation reported that the expression level of CX3CR1 was increased among individuals with more severe liver fibrosis[13], which is similar to this study showing poor prognosis in individuals with cirrhosis with higher expression of CX3CR1. Furthermore, serum levels of CX3CL1 in individuals with liver cirrhosis were considerably higher

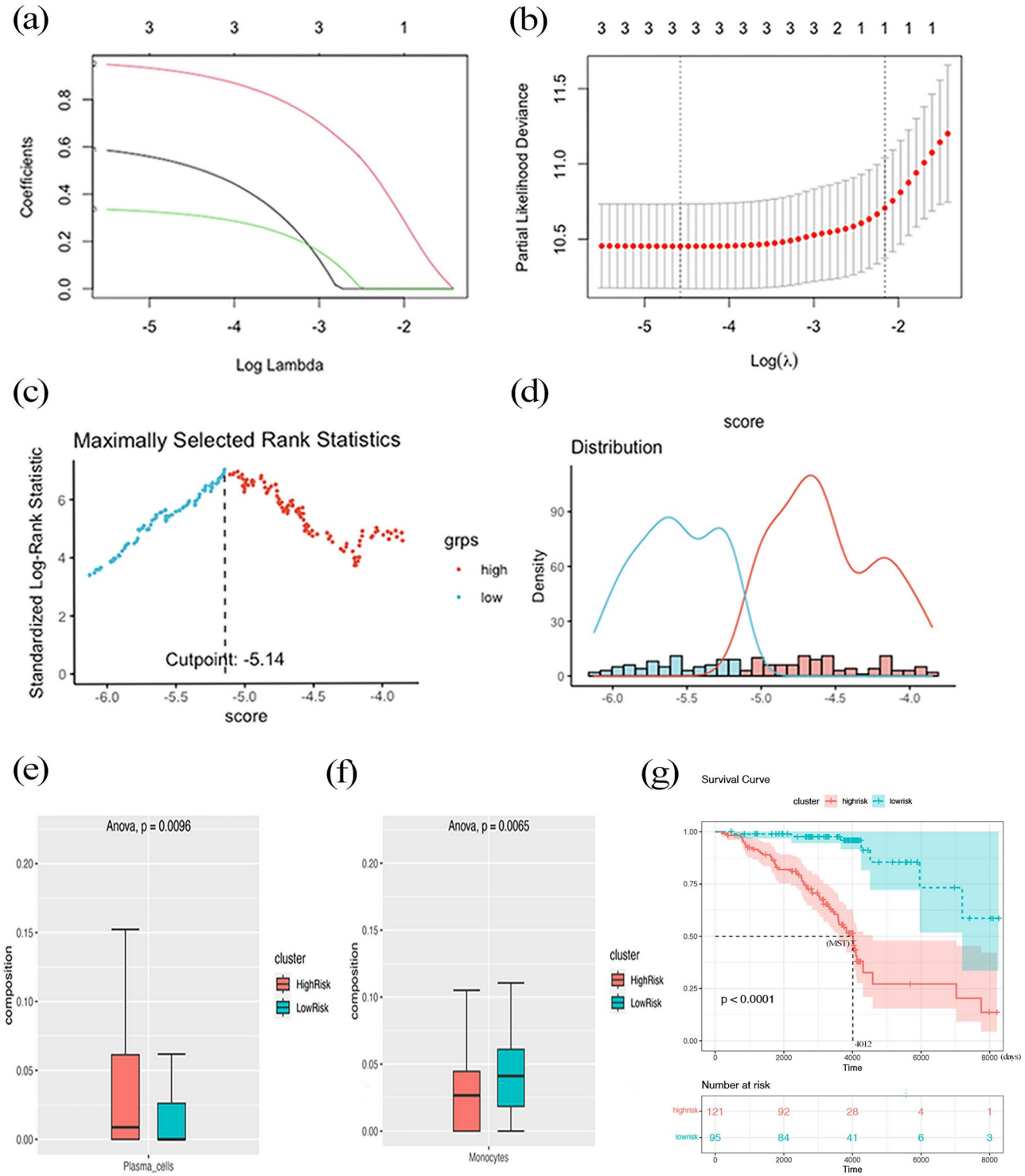

Fig. 5. (**a**) LASSO coefficient profiles of 3 risk models. (**b**) Three-fold cross-validation of lasso analysis. (**c**) Histogram based on maximally selected rank grouping in combined model. (**d**) Grouping cut-off value based on maximally selected rank. (**e**) The infiltration of plasma cells in two clusters based on the combined risk model. (**f**) The infiltration of monocytes in two clusters based on the combined risk model (**g**) Kaplan–Meier diagram of the total survival rate of combined risk model.

than those in healthy donors, positively correlating with their Child–Pugh score[21]. However, other studies emphasized that CX3CR1 plays an important role in protecting the body from inflammatory damage. For example, in the mice model of schistosomiasis hepatic cirrhosis, CX3CR1 expression was upregulated after *Schistosoma japonicum cercariae* infection[22]. In addition, CX3CR1 deficiency mitigated acute inflammation by fostering M2 macrophage polarization[23].

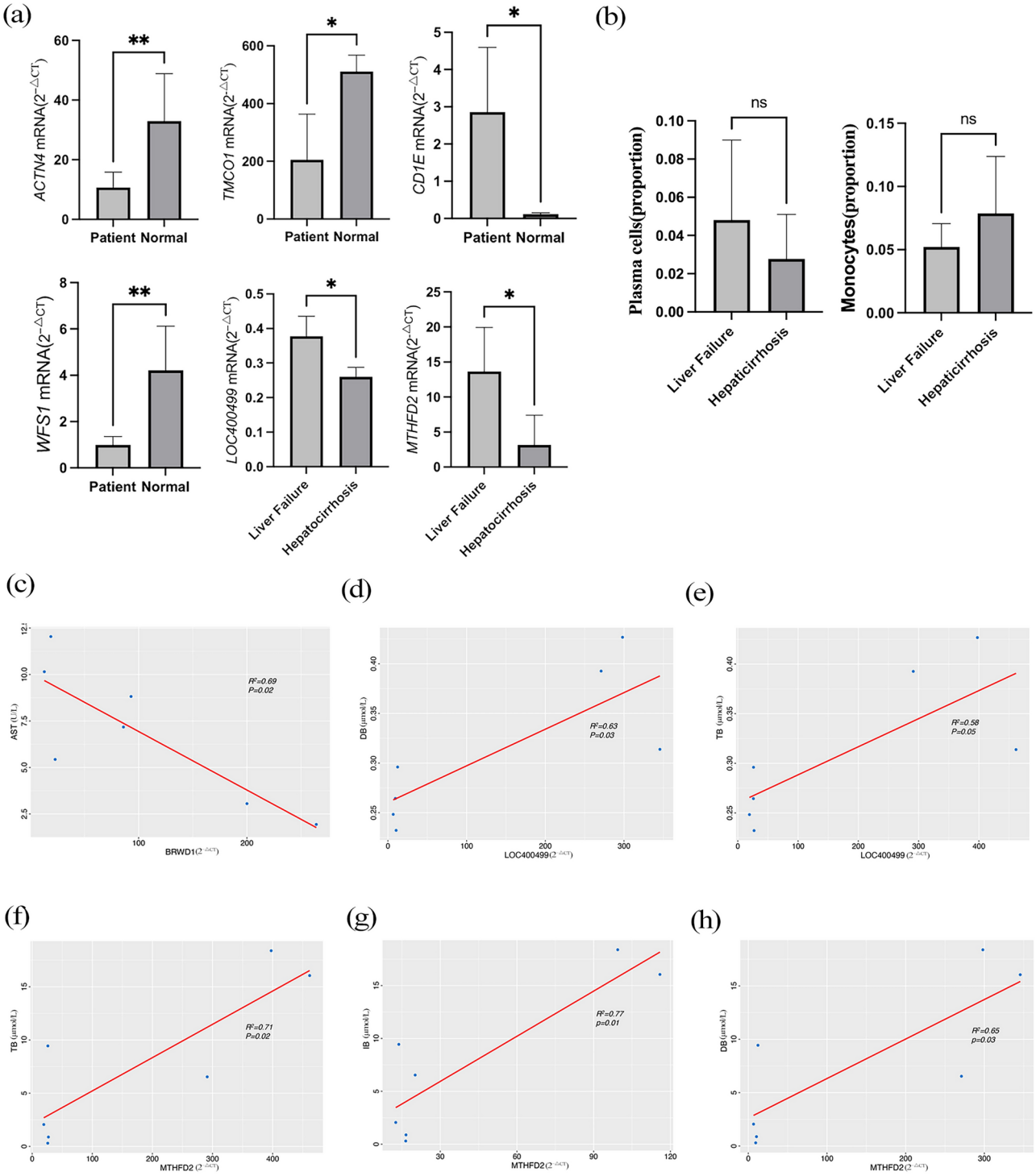

Fig. 6. (**a**) The expression of ACTN4, TMCO1, CD1E, WFS1 between liver donor and patients. The expression of LOC400499 and MTHFD2 between liver failure and hepatiocirrhosis patients. **means $P < 0.01$, *means $P < 0.05$. (**b**) The infiltration of monocytes and plasma cells in clinical samples. (**c**–**h**) Pearson analysis showed the correlation between gene expression and clinical features.

CX3CR1 contributes to the progression of liver fibrosis in several ways. The CX3CR1 coding variant V249I is strongly associated with advanced liver fibrosis. The presence of CX3CR1 in HSCs indicates that its interaction with fractalkine suppresses the expression of tissue inhibitor of matrix metalloproteinase 1 (TIMP1) mRNA in HSCs, thereby promoting the progression of liver cirrhosis[24]. Meanwhile, HMGB2 plays a crucial role in the activation of HSCs. In Hmgb2-/- mice, the activation of the CX3CR1 gene is significantly inhibited, leading to a reduction in fibrosis[25]. As liver fibrosis progresses, there is a notable expansion of CX3CR1 + monocyte-derived

Characteristics	Liver failure(n = 3)	Hepatocirrhosis(n = 4)
Serum albumin (g/L)	30.2 ± 5.8	37.8 ± 3.08
Prothrombin time (s)	16.67 ± 0.55	14.18 ± 1.91
Total bilirubin(μmol/L)	383.37 ± 70.28	24.58 ± 3.07
Direct bilirubin(μmol/L)	304.87 ± 31.87	9.70 ± 2.02
Indirect bilirubin (μmol/L)	78.50 ± 41.77	14.88 ± 1.73
Aspartate aminotransferase(U/L)	126.33 ± 52.17	79.75 ± 106.44
Hepatic encephalopathy	3	0
Ascites	3	2
Child–Pugh class B/C	3	0

Table 4. Clinical information of clinical samples.

inflammatory dendritic cells, which activate surrounding HSCs through the secretion of pro-inflammatory factors such as TNFα. This process results in excessive deposition of ECM and structural remodeling of the liver, further promoting the development of liver fibrosis[26]. Therefore, CX3CR1 is a critical mediator in the progression of liver fibrosis induced by HCV and holds potential as a therapeutic target for HCV-induced fibrosis. However, current research on the relationship between HCV and CX3CR1 is limited, underscoring the need for further investigation in this area.

The present study found a set of genes correlated with the expression of CX3CR1 and immune cell infiltration, including ACTN4, BRWD1, CD1E, HYPK, ITGB7, LOC400499, MTHFD2, THBS2, TMCO1, TMPRSS13, and WSF1. During validation, ACTIN4, CD1E, TMCO1, and WSF1 exhibited distinct expression in disease conditions. In contrast, LOC400499 and MTHFD2 showed elevated expression in liver failure tissues compared to hepatocirrhosis. In addition, expressions of LOC400499 and MTHFD2 were positively related to liver function, while the expression of BRWD1 was negatively correlated with liver function indices. ACTN4, also known as alpha-actinin 4, is critically involved in the pathogenesis of hepatocellular carcinoma (HCC), promoting cancer cell invasion, metastasis, and signaling regulation[27–29]. Although the role of ACTN4 in liver fibrosis is underreported at present, it's been associated with kidney fibrosis and glomerulosclerosis progression. Notably, decreased expression of ACTN4 could delay kidney fibrosis development[30–32]. In the liver, the expression of ACTN4 is primarily observed in cancer cells of HCC. Therefore, the main source of ACTN4 may still be hepatocytes[27–29]. ACTN4 interacts with AKT1 and enhances its phosphorylation[33]. The interaction between ACTN4 and TRIP13 in HCC activates the AKT/mTOR pathway, triggering EMT[29], a process significant to the progression of liver fibrosis. Recent studies have shown that CX3CR1 may play a role in various biological processes by regulating the AKT/mTOR pathway[34–36]. One study found that in hepatopulmonary syndrome caused by cirrhosis, the increased expression of CX3CL1 and CX3CR1 in the lungs stimulates AKT pathway activation, further promoting the accumulation of intrapulmonary monocytes, angiogenesis, and the development of experimental hepatopulmonary syndrome[34]. In our study, we found that CX3CR1 was positively correlated with ACTN4 in HCV-induced fibrosis, and high ACTN4 expression predicted poor prognosis. Therefore, we speculate that CX3CR1 and ACTN4 may co-participate in the progression of liver fibrosis through the AKT pathway. However, further research is needed. BRWD1, a bromodomain and WD repeat-containing protein 1 holds a predicted molecular weight of 263 KD and encompasses tandem BROMO domains and a WD40 repeat sequence[37]. Previously conducted studies have shown that the expression of BRWD1 is correlated with the development and maturation of sperm and eggs[38]. Meanwhile, the loss of BRWD1 has been correlated with the incidence of Down syndrome and hypogammaglobulinemia[39,40]. BRWD1 is highly expressed in follicular B cells and plays a crucial role in B lymphocyte development and immune regulation. It functions by closing early developmental enhancers in small pre-B cells while opening enhancers associated with late B lymphopoiesis to promote transcription factor binding. The expression and recruitment of BRWD1 are regulated by stage-specific signals, particularly the necessary inhibitory role of STAT5 during different stages of B cell development[39,41]. The loss of CX3CR1 results in reduced proximal BCR signaling while enhancing the activation of distal signaling pathways related to metabolic reprogramming. Additionally, CX3CR1 deficiency leads to overactivation of WASP and diminished dephosphorylation of Ezrin in small pre-B cells, affecting BCR clustering and signalosome recruitment[42]. This impact may intertwine with BRWD1's role in regulating enhancer accessibility, suggesting that BRWD1 might play a role in the signaling changes mediated by CX3CR1 through its regulation of transcriptional programs related to B cell development. At present, no research has discussed the role of BRWD1 in liver or fibrosis diseases. Our study found that the expression of BRWD1 had negative correlation with CX3CR1 in HCV-induced cirrhosis. The potential interaction between CX3CR1 and BRWD1 warrants further investigation to better understand their collaborative effects on B cell development and liver fibrosis. CD1E, a member of the CD1 family, is a membrane-associated protein located in the Golgi compartment of immature human dendritic cells. It is subsequently transported to lysosomes, where it is cleaved into soluble form. CD1E is involved in glycolipid antigen processing[43]. Expression of CD1E is also detected on T cell membranes, facilitating glycolipid antigen presentation on the cell surface[44]. Studies involving CD1E have been reported in conditions such as HCC, chronic lung allograft dysfunction, and multiple sclerosis[45–47]. High expression of CD1E indicated poor prognosis in individuals with HCC due to altered lipid microenvironment[47]. This study suggested that CD1E had positive correlation with the expression of CX3CR1 and predicted poor prognosis in individuals with cirrhosis. While no studies reported a link between CD1E expression and fibrosis,

the progression of liver fibrosis is closed associated with the innate and adaptive immune responses mediated by T cells and dendritic cells. Compared to healthy individuals, CD1c + DCs, which belong to the CD1 family along with CD1e, exhibit a significant reduction in their ability to kill target cells in patients with chronic hepatitis C[48]. Additionally, in renal fibrosis, CD1c + DCs serve as a primary source of TGF-β and CX3CR1 expression. The secretion of CX3CL1 by proximal tubular epithelial cells induces the accumulation of TGF-β-producing CD1c + DCs in the renal interstitium, promoting the progression of fibrotic diseases[49]. However, the precise mechanism between CD1E and CX3CR1 necessitates further research. TMCO1, a product of transmembrane and coiled-coil domains 1, belongs to the DUF841 superfamily[50]. This multifunctional eukaryotic protein plays a crucial role in preventing excessive intracellular Ca^{2+} accumulation and maintaining endoplasmic reticulum(ER) calcium homeostasis[51]. TMCO1 dysfunction is linked to various human diseases, including dysmorphism, mental retardation, glaucoma, tumorigenesis, gliomas, and osteoporosis[52,53]. TMCO1 mRNA widely expressed in liver[50]. The interaction of CX3CL1 with CX3CR1 increases Ca^{2+} levels, which activates Calcium/calmodulin-dependent Protein Kinase II delta (CaMKIIδ) and prompts the translocation of HDAC4 from the nucleus to the cytosol. This translocation inhibits autophagy in Kupffer cells, leading to their apoptosis and contributing to liver damage[54]. Furthermore, a study revealed that the absence of TMCO1 resulted in reduced CaMKII phosphorylation, which in turn decreased HDAC4 phosphorylation, ultimately impairing bone formation and osteoblast differentiation[52]. Our study suggested that high expression of TMCO1 indicated better prognosis in patients with cirrhosis. In the context of liver fibrosis, the high expression of CX3CR1 may lead to increased Ca^{2+} levels, which in turn reduces the expression of TMCO1, thereby maintaining intracellular Ca^{2+} homeostasis. The process may be mediated by the CaMKIIδ/HDAC4 axis involving both factors. The transmembrane protein wolframin, encoded by the nuclear gene WSF1, resides in the ER membrane. WSF1 mutations are associated with Wolfram syndrome or type 2 diabetes mellitus[55]. WFS1-encoded wolframin could play a role by maintaining the body's calcium levels in conjunction with CX3CR1 in fibrosis. The deficiency of WFS1 disrupts communication between the ER and mitochondria within specialized suborganelles known as mitochondria-associated ER membranes (MAMs), resulting in mitochondrial dysfunction[56]. HCV proteins specifically associate with MAMs, which are essential for viral replication[57]. Therefore, the reduced expression of MAMs due to WFS1 deficiency may influence the progression of HCV-induced fibrosis. Moreover, this research demonstrated a positive relationship between the expression of LOC400499 and MTHFD2 and the clinical signature of patients. The LOC400499 gene remains unidentified. Our study suggested that LOC400499 is positively correlated with the progression of liver fibrosis in patients. Methylenetetrahydrofolate dehydrogenase 2 (MTHFD2) is a key enzyme in one-carbon metabolism. A study linked the high expression of MTHFD2 to lung fibrosis development in mice[58]. In addition, MTHFD2 is overexpressed in HCC, and its deficiency showed potential antitumor effects in various cancers[59]. In HCC, Wnt/beta-catenin signaling pathway regulates the expression of MTHFD2. Suppressed expression of MTHFD2 considerably attenuated the malignant phenotype of tumor cells induced by the activation of the Wnt/beta-catenin signaling pathway[60]. Wnt/β-catenin is one of the important signaling pathways through which the CX3CL1/CX3CR1 axis influences the inflammatory process[36]. Therefore, CX3CR1 may interact with MTHFD2 to modulate the inflammatory response and disease progression by influencing the Wnt/β-catenin signaling pathway.

The innate and adaptive immune systems perform a critical function in the process of liver fibrosis, promoting the activation of hepatic stellate cells and subsequent ECM deposition. The present study characterized the immune cell composition linked to the expression of CX3CR1-associated genes and its prognostic value in individuals with HCV-induced early-stage liver cirrhosis. Monocytes recruited from the peripheral blood through the CX3CR1–CX3CL1 axis differentiate into macrophages[61] that centrally govern the progression and regression of liver cirrhosis through their phenotypic changes. The combined model revealed that higher monocyte infiltration predicts a better prognosis. Previous studies have reported that CX3CR1 can limit liver cirrhosis by controlling the differentiation and survival of intrahepatic monocytes[14,62]. Consequently, inhibiting monocyte-to-proinflammatory macrophage differentiation might emerge as a viable strategy to reverse cirrhosis. Furthermore, this study showed that infiltration of plasma cells in injured livers was correlated with a worse prognosis. Plasma cells are a terminally differentiated form of B cells. B cells account for nearly half of the lymphocyte population in the liver[63]. In chronic liver disease, retinoic acid produced by HSCs enhances B cell survival, expression of the plasma cell marker CD138, and IgG production, thereby exacerbating liver fibrosis progression[64]. Additionally, the involvement of B cells in αCD40-induced necrotizing inflammatory liver disease reveals their pro-inflammatory role, which is dependent on the presence of macrophages[65]. In addition, infiltration of follicular helper T cells was found to be a prognostic risk factor for individuals with liver cirrhosis. Although its role in recruiting eosinophils during schistosomiasis infection has been reported, scarce attention has been paid to its role in liver cirrhosis pathogenesis[66].

There are several limitations to this study. First, the analysis was based on a retrospective cohort with individuals exclusively suffering from chronic HCV infection, potentially limiting the direct applicability of these findings to cirrhosis resulting from other causes such as chronic HBV infection or non-alcoholic fatty liver disease. Second, the clinical sample size was relatively small, preventing the verification of all gene expressions. Third, this study was unable to assess the relationship between liver immune infiltration and systemic immune status in individuals with cirrhosis due to the absence of fresh samples from patients. In future studies, it is intended to expand the sample size and investigate the mechanism underlying CX3CR1-associated genes in liver fibrosis. In addition, the aim is to compare data from HC, individuals who are decompensated, and those with acute-on-chronic liver failure with individuals in the early stage to precisely delineate the role of CX3CR1 and its associated immune cells in liver cirrhosis pathogenesis.

In summary, the current research explored the prognostic value of CX3CR1 in individuals with chronic HCV infection and examined its correlation with immune cell infiltration using bioinformatic analyses. An integrated prognostic model based on the expression of CX3CR1, CX3CR1-associated IIGs, and immune infiltration

pattern was constructed to predict patient outcomes. Furthermore, clinical samples collected from healthy liver donors, individuals with post-hepatic cirrhosis, and those with acute-on-chronic liver failure were verified using the bioinformatics findings. In conclusion, these findings suggest that CX3CR1 could emerge as a novel target for mitigating and managing the progression of liver cirrhosis.

Material and methods

Dataset preparation

The microarray expression dataset GSE15654 was acquired from the Gene Expression Omnibus (GEO) database (https://www.ncbi.nlm.nih.gov/gds)[67]. This dataset encompassed 216 individuals with HCV-related early-stage cirrhosis from an Italian center, with a median follow-up duration of 10 years. Using the platform annotation file, probes within the dataset were converted into corresponding gene symbols. Duplicate probes were excluded from the dataset, retaining the maximum value, before performing log2 normalization.

Identification of CX3CR1 as a risk factor in individuals with liver cirrhosis

The expression matrix of CX3CR1 was extracted, and the maximally selected rank statistics were employed to divide the individuals into high and low-risk groups (categories). The algorithm was implemented using the R packages "survival" and "survminer." Combined with the clinical information, the Kaplan–Meier method was utilized to create risk model 1.

Identification of CX3CR1-associated genes in individuals with liver cirrhosis

To gain further clarity regarding genes associated with disease progression, univariate Cox analysis was employed across the whole genome, retaining genes with $P < 0.05$. Pearson correlation analysis was conducted to identify genes related to CX3CR1 (|Pearson R|> 0.2 and $P < 0.05$). Subsequently, gene ontology functional annotation (GO) and Kyoto Encyclopedia of Genes and Genomes analyses (KEGG) were employed to uncover the functional roles and signaling pathways of the CX3CR-associated genes. The GO and KEGG analyses were performed using "DAVID" available at https://david.ncifcrf.go. Adjusted $P < 0.05$ was considered statistically significant. The GO enrichment plot and KEGG bubble chart were generated using the online tool at http://www.sangerbox.com.

Identification of immune infiltration patterns in individuals with liver cirrhosis

CIBERSORT analysis was employed to determine the composition of 22 immune cell types in individuals with liver cirrhosis. Using Pearson correlation analysis, genes linked to immune cell infiltration were selected from CX3CR1-associated genes (|Pearson R|> 0.2 and $P < 0.05$). Subsequently, these genes were identified as CX3CR1-associated IIGs. The least absolute shrinkage and selection operator (LASSO), a type of shrinkage-based linear regression, was employed to filtrate the optimal gene set. Multivariate Cox regression analysis was conducted to determine corresponding coefficients. The risk score for CX3CR1-associated IIGs was calculated as Score = ∑i 1n (Coefi ∗ the expression of a relative gene). A coefficient exceeding 0 indicated a risk factor, while values below 0 indicated a protective factor. Using the risk score, maximally selected rank statistics were utilized to categorize individuals into two clusters. Survival curves were generated for predicting the survival differences between the two clusters (risk model 2).

Identification of CX3CR1-associated immune infiltration cells in individuals with liver cirrhosis

Immune cells that exhibited correlation with CX3CR1-associated genes were isolated using Pearson correlation analysis. These cells were then designated as CX3CR1-associated IIGs. Subsequently, individuals were divided into high- and low-immune infiltration clusters as per the infiltration levels of the identified immune cells, employing maximally selected rank statistics. The survival curve was utilized to ascertain the impact of CX3CR1-associated immune infiltration cells on the survival duration of individuals with liver cirrhosis (risk model 3).

Integrated prognostic model for individuals with liver cirrhosis

Based on the risk scores of CX3CR1, CX3CR1-associated IIGs, and CX3CR1-associated immune infiltration cells, an integrated prognostic model for liver cirrhosis was developed. This model entailed calculating the combined risk score as Score = ∑i 1n (Coefi ∗ corresponding risk score), with coefficients established using multivariate Cox regression analysis. Employing the combined risk score, maximally selected rank statistics were used to classify individuals into high- and low-risk groups. The Kaplan–Meier method was then applied to create a survival curve.

Validation of clinical patients

To verify the aforementioned bioinformatic findings, 10 surgical resection specimens, including 3 healthy controls (HC), 4 individuals with HCV-induced hepatic cirrhosis, and 3 with HCV-induecd liver failure, were collected for gene expression testing. The research was approved by the institutional review board (Ethics Committee) of the West China Hospital of Sichuan University (2023-288). RNA was extracted from the liver tissues using TRIzol reagent, followed by quantitative reverse transcriptase-PCR (qRT-PCR) to assess the expression of CX3CR1-associated IIGs. Each gene was evaluated three times, and the mean cycle threshold data was computed. Equation $2^{-\triangle CT}$ was used to ascertain relative gene expression.

RNA-seq analysis of clinical samples

Seven liver fibrosis clinical samples were analysed by RNA-seq. Total RNA was isolated from liver specimens using an RNA Isolation Kit (Foregene, Chengdu, China). RNA-sequencing (RNA-seq) libraries were constructed

and sequenced using the Illumina NovaSeq™ X Plus platform, with the process carried out by Anoroad (Beijing, China). The evaluation of relative gene expression was based on transcripts per million (TPM).

Statistical analysis

All analyses were executed using R 4.0.2 and Graphpad Prism 9.0. The maximally selected rank statistics algorithm and survival plots were generated using the R packages "survival" and "survminer." CIBERSORT analysis was conducted at https://cibersort.stanford.edu/. The LASSO and Cox regression models were developed using the R package "glmnet." PCR results were presented as mean ± standard deviation. Continuous data were compared utilizing the unpaired t-test. The code used in this study has been uploaded as Supplementary Material 1.

Data availability

The datasets generated and/or analysed during the current study are available are publicly available. The data can be found here: Gene Expression Omnibus GEO, available at: https://www.ncbi.nlm.nih.gov/geo/query/acc.cgi?acc=GSE15654.

Received: 28 April 2024; Accepted: 19 November 2024
Published online: 13 January 2025

References

1. Huang, D. Q. et al. Global epidemiology of cirrhosis—Aetiology, trends and predictions. *Nat. Rev. Gastroenterol. Hepatol.* https://doi.org/10.1038/s41575-023-00759-2 (2023).
2. Jepsen, P. & Younossi, Z. M. The global burden of cirrhosis: A review of disability-adjusted life-years lost and unmet needs. *J. Hepatol.* https://doi.org/10.1016/j.jhep.2020.11.042 (2021).
3. Hernandez-Gea, V. & Friedman, S. L. Pathogenesis of liver fibrosis. *Ann. Rev. Pathol.* **6**, 425–456. https://doi.org/10.1146/annurev-pathol-011110-130246 (2011).
4. Manns, M. P. et al. Hepatitis C virus infection. *Nat. Rev. Dis. Primers* **3**, 17006. https://doi.org/10.1038/nrdp.2017.6 (2017).
5. Manns, M. P. & Maasoumy, B. Breakthroughs in hepatitis C research: From discovery to cure. *Nat. Rev. Gastroenterol. Hepatol.* **19**, 533–550. https://doi.org/10.1038/s41575-022-00608-8 (2022).
6. Zhang, Y., Chen, L. M. & He, M. Hepatitis C Virus in mainland China with an emphasis on genotype and subtype distribution. *Virol. J.* **14**, 41. https://doi.org/10.1186/s12985-017-0710-z (2017).
7. Vo-Quang, E. & Pawlotsky, J. M. "Unusual" HCV genotype subtypes: Origin, distribution, sensitivity to direct-acting antiviral drugs and behaviour on antiviral treatment and retreatment. *Gut* **73**, 1570–1582. https://doi.org/10.1136/gutjnl-2024-332177 (2024).
8. Ginès, P. et al. Liver cirrhosis. *Lancet (London, England)* **398**, 1359–1376. https://doi.org/10.1016/S0140-6736(21)01374-X (2021).
9. Ginès, P. et al. Population screening for liver fibrosis: Toward early diagnosis and intervention for chronic liver diseases. *Hepatology (Baltimore, Md)* **75**, 219–228. https://doi.org/10.1002/hep.32163 (2022).
10. Caraceni, P., Abraldes, J. G., Ginès, P., Newsome, P. N. & Sarin, S. K. The search for disease-modifying agents in decompensated cirrhosis: From drug repurposing to drug discovery. *J. Hepatol.* **75**(Suppl 1), S118–S134. https://doi.org/10.1016/j.jhep.2021.01.024 (2021).
11. Imai, T. et al. Identification and molecular characterization of fractalkine receptor CX3CR1, which mediates both leukocyte migration and adhesion. *Cell* **91**, 521–530 (1997).
12. Cai, H. et al. The combined model of CX3CR1-related immune infiltration genes to evaluate the prognosis of idiopathic pulmonary fibrosis. *Front. Immunol.* **13**, 837188. https://doi.org/10.3389/fimmu.2022.837188 (2022).
13. Wasmuth, H. E. et al. The fractalkine receptor CX3CR1 is involved in liver fibrosis due to chronic hepatitis C infection. *J. Hepatol.* **48**, 208–215 (2008).
14. Karlmark, K. R. et al. The fractalkine receptor CX_3CR1 protects against liver fibrosis by controlling differentiation and survival of infiltrating hepatic monocytes. *Hepatology (Baltimore, Md.)* **52**, 1769–1782. https://doi.org/10.1002/hep.23894 (2010).
15. Kisseleva, T. & Brenner, D. Molecular and cellular mechanisms of liver fibrosis and its regression. *Nat. Rev. Gastroenterol. Hepatol.* **18**, 151–166. https://doi.org/10.1038/s41575-020-00372-7 (2021).
16. Tsuchida, T. & Friedman, S. L. Mechanisms of hepatic stellate cell activation. *Nat. Rev. Gastroenterol. Hepatol.* **14**, 397–411. https://doi.org/10.1038/nrgastro.2017.38 (2017).
17. Ramachandran, P. et al. Resolving the fibrotic niche of human liver cirrhosis at single-cell level. *Nature* **575**, 512–518. https://doi.org/10.1038/s41586-019-1631-3 (2019).
18. Mizutani, S. et al. Treatment with an Anti-CX3CL1 antibody suppresses M1 macrophage infiltration in interstitial lung disease in SKG mice. *Pharmaceuticals (Basel, Switzerland)* https://doi.org/10.3390/ph14050474 (2021).
19. Helmke, A. et al. CX3CL1-CX3CR1 interaction mediates macrophage-mesothelial cross talk and promotes peritoneal fibrosis. *Kidney Int.* **95**, 1405–1417. https://doi.org/10.1016/j.kint.2018.12.030 (2019).
20. Kanehisa, M. & Goto, S. KEGG: Kyoto encyclopedia of genes and genomes. *Nucleic Acids Res.* **28**, 27–30. https://doi.org/10.1093/nar/28.1.27 (2000).
21. Qiao, G. et al. Serum fractalkine levels were positively associated with disease severity of liver cirrhosis. *Ann. Clin. Lab. Sci.* **51**, 844–851 (2021).
22. Zhang, P., Wang, B.-J., Wang, J.-Z., Xie, X.-M. & Tong, Q.-X. Association of CX3CL1 and CX3CR1 expression with liver fibrosis in a mouse model of schistosomiasis. *Curr. Med. Sci.* **40**, 1121–1127. https://doi.org/10.1007/s11596-020-2294-x (2020).
23. Ran, L. et al. Cx3cr1 deficiency in mice attenuates hepatic granuloma formation during acute schistosomiasis by enhancing the M2-type polarization of macrophages. *Dis. Models Mech.* **8**, 691–700. https://doi.org/10.1242/dmm.018242 (2015).
24. Wasmuth, H. E. et al. The fractalkine receptor CX3CR1 is involved in liver fibrosis due to chronic hepatitis C infection. *J. Hepatol.* **48**, 208–215. https://doi.org/10.1016/j.jhep.2007.09.008 (2008).
25. Huang, Y. et al. HMGB2 is a potential diagnostic marker and therapeutic target for liver fibrosis and cirrhosis. *Hepatol. Commun.* https://doi.org/10.1097/hc9.0000000000000299 (2023).
26. Sutti, S. et al. CX3CR1-expressing inflammatory dendritic cells contribute to the progression of steatohepatitis. *Clin. Sci. (Lond)* **129**, 797–808. https://doi.org/10.1042/cs20150053 (2015).
27. Chen, Q. et al. Circular RNA ACTN4 promotes intrahepatic cholangiocarcinoma progression by recruiting YBX1 to initiate FZD7 transcription. *J. Hepatol.* **76**, 135–147. https://doi.org/10.1016/j.jhep.2021.08.027 (2022).
28. Bi, Q. et al. MTBP inhibits migration and metastasis of hepatocellular carcinoma. *Clin. Exp. Metastasis* **32**, 301–311. https://doi.org/10.1007/s10585-015-9706-5 (2015).
29. Zhu, M. X. et al. Elevated TRIP13 drives the AKT/mTOR pathway to induce the progression of hepatocellular carcinoma via interacting with ACTN4. *J. Exp. Clin. Cancer Res.* **38**, 409. https://doi.org/10.1186/s13046-019-1401-y (2019).

30. He, C. et al. Epigallocatechin gallate induces the demethylation of actinin alpha 4 to inhibit diabetic nephropathy renal fibrosis via the NF-KB signaling pathway in vitro. *Dose Response* **20**, 15593258221105704. https://doi.org/10.1177/15593258221105704 (2022).
31. He, S. et al. Reversible SAHH inhibitor protects against glomerulonephritis in lupus-prone mice by downregulating renal α-actinin-4 expression and stabilizing integrin-cytoskeleton linkage. *Arthritis. Res. Ther.* **21**, 40. https://doi.org/10.1186/s13075-019-1820-3 (2019).
32. Zhang, M., Liu, S., Fang, L., Wang, G. & Yin, L. Asiaticoside inhibits renal fibrosis development by regulating the miR-142-5p/ACTN4 axis. *Biotechnol. Appl. Biochem.* **69**, 313–322. https://doi.org/10.1002/bab.2110 (2022).
33. Ding, Z. et al. A retrovirus-based protein complementation assay screen reveals functional AKT1-binding partners. *Proc. Natl. Acad. Sci. U. S. A.* **103**, 15014–15019. https://doi.org/10.1073/pnas.0606917103 (2006).
34. Zhang, J. et al. The role of CX_3CL1/CX_3CR1 in pulmonary angiogenesis and intravascular monocyte accumulation in rat experimental hepatopulmonary syndrome. *J. Hepatol.* **57**, 752–758. https://doi.org/10.1016/j.jhep.2012.05.014 (2012).
35. Klosowska, K. et al. Fractalkine functions as a chemoattractant for osteoarthritis synovial fibroblasts and stimulates phosphorylation of mitogen-activated protein kinases and Akt. *Clin. Exp. Immunol.* **156**, 312–319. https://doi.org/10.1111/j.1365-2249.2009.03903.x (2009).
36. Zhuang, Q., Ou, J., Zhang, S. & Ming, Y. Crosstalk between the CX3CL1/CX3CR1 axis and inflammatory signaling pathways in tissue injury. *Curr. Protein Pept. Sci.* **20**, 844–854. https://doi.org/10.2174/1389203720666190305165722 (2019).
37. Huang, H., Rambaldi, I., Daniels, E. & Featherstone, M. Expression of the Wdr9 gene and protein products during mouse development. *Dev. Dyn.* **227**, 608–614. https://doi.org/10.1002/dvdy.10344 (2003).
38. Pattabiraman, S. et al. Mouse BRWD1 is critical for spermatid postmeiotic transcription and female meiotic chromosome stability. *J. Cell Biol.* **208**, 53–69. https://doi.org/10.1083/jcb.201404109 (2015).
39. Mandal, M. et al. BRWD1 orchestrates epigenetic landscape of late B lymphopoiesis. *Nat. Commun.* **9**, 3888. https://doi.org/10.1038/s41467-018-06165-6 (2018).
40. Fulton, S. L. et al. Rescue of deficits by Brwd1 copy number restoration in the Ts65Dn mouse model of Down syndrome. *Nat. Commun.* **13**, 6384. https://doi.org/10.1038/s41467-022-34200-0 (2022).
41. Mandal, M. et al. Histone reader BRWD1 targets and restricts recombination to the Igk locus. *Nat. Immunol.* **16**, 1094–1103. https://doi.org/10.1038/ni.3249 (2015).
42. Li, N. et al. CX3CR1 positively regulates BCR signaling coupled with cell metabolism via negatively controlling actin remodeling. *Cell Mol. Life Sci.* **77**, 4379–4395. https://doi.org/10.1007/s00018-019-03416-7 (2020).
43. Tang, Y. et al. Cell-free protein synthesis of CD1E and B2M protein and in vitro interaction. *Protein Expr. Purif.* **203**, 106209. https://doi.org/10.1016/j.pep.2022.106209 (2023).
44. Maitre, B. et al. Control of the intracellular pathway of CD1e. *Traffic* **9**, 431–445. https://doi.org/10.1111/j.1600-0854.2008.00707.x (2008).
45. Parkes, M. D. et al. Transcripts associated with chronic lung allograft dysfunction in transbronchial biopsies of lung transplants. *Am. J. Transplant.* **22**, 1054–1072. https://doi.org/10.1111/ajt.16895 (2022).
46. Caporale, C. M. et al. CD1A and CD1E gene polymorphisms are associated with susceptibility to multiple sclerosis. *Int. J. Immunopathol. Pharmacol.* **24**, 175–183. https://doi.org/10.1177/039463201102400120 (2011).
47. Fessas, P. et al. Phenotypic characteristics of the tumour microenvironment in primary and secondary hepatocellular carcinoma. *Cancers (Basel)* https://doi.org/10.3390/cancers13092137 (2021).
48. Ciesek, S. et al. Impaired TRAIL-dependent cytotoxicity of CD1c-positive dendritic cells in chronic hepatitis C virus infection. *J. Viral Hepat.* **15**, 200–211. https://doi.org/10.1111/j.1365-2893.2007.00930.x (2008).
49. Kassianos, A. J. et al. Fractalkine-CX3CR1-dependent recruitment and retention of human CD1c+ myeloid dendritic cells by in vitro-activated proximal tubular epithelial cells. *Kidney Int.* **87**, 1153–1163. https://doi.org/10.1038/ki.2014.407 (2015).
50. Zhang, Z. et al. Molecular cloning, expression patterns and subcellular localization of porcine TMCO1 gene. *Mol. Biol. Rep.* **37**, 1611–1618. https://doi.org/10.1007/s11033-009-9573-8 (2010).
51. Wang, Q. C. et al. TMCO1 Is an ER Ca(2+) Load-Activated Ca(2+) Channel. *Cell* **165**, 1454–1466. https://doi.org/10.1016/j.cell.2016.04.051 (2016).
52. Li, J. et al. TMCO1-mediated Ca(2+) leak underlies osteoblast functions via CaMKII signaling. *Nat. Commun.* **10**, 1589. https://doi.org/10.1038/s41467-019-09653-5 (2019).
53. Gao, L. et al. TMCO1 expression promotes cell proliferation and induces epithelial-mesenchymal transformation in human gliomas. *Med. Oncol.* **39**, 90. https://doi.org/10.1007/s12032-022-01687-y (2022).
54. Li, Y. et al. CX3CL1 represses autophagy via CX3CR1/CaMKIIδ/HDAC4/Rubicon axis and exacerbates chronic intermittent hypoxia induced Kupffer cell apoptosis. *Cell Signal* **111**, 110873. https://doi.org/10.1016/j.cellsig.2023.110873 (2023).
55. de Muijnck, C., Brink, J. B. T., Bergen, A. A., Boon, C. J. F. & van Genderen, M. M. Delineating Wolfram-like syndrome: A systematic review and discussion of the WFS1-associated disease spectrum. *Surv. Ophthalmol.* https://doi.org/10.1016/j.survophthal.2023.01.012 (2023).
56. Crouzier, L. et al. Activation of the sigma-1 receptor chaperone alleviates symptoms of Wolfram syndrome in preclinical models. *Sci. Transl. Med.* **14**, eabh3763. https://doi.org/10.1126/scitranslmed.abh3763 (2022).
57. Duponchel, S. et al. Hepatitis C virus replication requires integrity of mitochondria-associated ER membranes. *JHEP Rep.* **5**, 100647. https://doi.org/10.1016/j.jhepr.2022.100647 (2023).
58. Snyder-Talkington, B. N. et al. mRNAs and miRNAs in whole blood associated with lung hyperplasia, fibrosis, and bronchiolo-alveolar adenoma and adenocarcinoma after multi-walled carbon nanotube inhalation exposure in mice. *J. Appl. Toxicol.* **36**, 161–174. https://doi.org/10.1002/jat.3157 (2016).
59. Liu, X. et al. Methylenetetrahydrofolate dehydrogenase 2 overexpression is associated with tumor aggressiveness and poor prognosis in hepatocellular carcinoma. *Dig. Liver Dis.* **48**, 953–960. https://doi.org/10.1016/j.dld.2016.04.015 (2016).
60. Ren, X. et al. The protein kinase activity of NME7 activates Wnt/β-catenin signaling to promote one-carbon metabolism in hepatocellular carcinoma. *Cancer Res.* **82**, 60–74. https://doi.org/10.1158/0008-5472.Can-21-1020 (2022).
61. Aspinall, A. I. et al. CX(3)CR1 and vascular adhesion protein-1-dependent recruitment of CD16(+) monocytes across human liver sinusoidal endothelium. *Hepatology (Baltimore, Md.)* **51**, 2030–2039. https://doi.org/10.1002/hep.23591 (2010).
62. Ni, Y. et al. CX3CL1/CX3CR1 interaction protects against lipotoxicity-induced nonalcoholic steatohepatitis by regulating macrophage migration and M1/M2 status. *Metab. Clin. Exp.* **136**, 155272. https://doi.org/10.1016/j.metabol.2022.155272 (2022).
63. Seki, E. & Schwabe, R. F. Hepatic inflammation and fibrosis: Functional links and key pathways. *Hepatology* **61**, 1066–1079. https://doi.org/10.1002/hep.27332 (2015).
64. Thapa, M. et al. Liver fibrosis occurs through dysregulation of MyD88-dependent innate B-cell activity. *Hepatology (Baltimore, Md.)* **61**, 2067–2079. https://doi.org/10.1002/hep.27761 (2015).
65. Kimura, K. et al. Pathogenic role of B cells in anti-CD40-induced necroinflammatory liver disease. *Am J Pathol* **168**, 786–795. https://doi.org/10.2353/ajpath.2006.050314 (2006).
66. Chen, X. et al. Follicular helper T cells recruit eosinophils into host liver by producing CXCL12 during *Schistosoma japonicum* infection. *J. Cell. Mol. Med.* **24**, 2566–2572. https://doi.org/10.1111/jcmm.14950 (2020).
67. Hoshida, Y. et al. Prognostic gene expression signature for patients with hepatitis C-related early-stage cirrhosis. *Gastroenterology* **144**, 1024–1030. https://doi.org/10.1053/j.gastro.2013.01.021 (2013).

Acknowledgements
None.

Author contributions
HC and JZ collected the literatures and drafted the initial manuscript. TW, CW and HC revised the manuscript and edited the language. WT conceptualized and guaranteed the review.CL, JS and XZ designed the figures and tables. WP, JZ and HL formatted the references and whole manuscript. All authors contributed to the article and approved the submitted version. HC and JZ contributed to this paper equally.

Funding
This study was supported by grants from the National Natural Science Foundation of China (No. 82070625, No. 82100650), and Technological Supports Project of Sichuan Province (No.2022YFS0257).

Declarations

Competing interests
The authors declare no competing interests.

Ethics declarations and approval for human experiments
The experimental protocol was established according to the ethical guidelines of the Helsinki Declaration. It was approved by the Human Ethics Committee of West China Hospital, Sichuan University (2023–288). Written informed consent was obtained from individual participants or their guardians.

Consent for publication
Not applicable.

Additional information
Supplementary Information The online version contains supplementary material available at https://doi.org/10.1038/s41598-024-80422-1.

Correspondence and requests for materials should be addressed to T.W.

Reprints and permissions information is available at www.nature.com/reprints.

Publisher's note Springer Nature remains neutral with regard to jurisdictional claims in published maps and institutional affiliations.